

1 Title : Variability of quantal NMDA to AMPA current ratio in nucleus tractus solitarii neurons

2

3

4

5 Authors : Caroline Strube¹, Florian Gackière^{1*}, Loyal Saliba¹, Fabien Tell¹ and Jean-Pierre Kessler^{1,2}

6

7

8 Author's affiliation :

9 ¹ Aix Marseille Université, CNRS, CRN2M UMR 7286, Marseille, France

10 ² Aix Marseille Université, CNRS, IBDM UMR 7288, Marseille, France

11

12

13 * :Present address : Neuroservice, Domaine de Saint Hilaire, 595 rue Pierre Berthier, CS 30531–13593

14 Aix en Provence cedex 03, France

15

16

17 Corresponding author : Jean-pierre Kessler

18 IBDM, UMR 7288 CNRS, Case 907, Parc Scientifique de Luminy, 13009 Marseille.

19 Email : jean-pierre.kessler@univ-amu.fr.

1

20 **Abstract**

21 The ratio between AMPA and NMDA receptors is a key factor governing integrative and plastic
22 properties of excitatory glutamatergic synapses. To determine whether the respective proportions of
23 AMPA and NMDA receptors are similar or vary across a neuron's synapse, we analyzed the variability
24 of NMDA and AMPA currents in quantal responses recorded from neurons located in the nucleus
25 tractus solitarii. We found that the average NMDA to AMPA current ratio strongly differed between
26 recorded neurons and that most of the intra-neuronal current ratio variability was attributable to
27 fluctuations in NMDA current. We next performed computer simulations with a Monte Carlo model of
28 a glutamatergic synapse to estimate the part of AMPA and NMDA currents fluctuations induced by
29 stochastic factors. We found that NMDA current variability mainly resulted from strong channel noise
30 with few influence of release variations. On the contrary, partly because of the presence of
31 subconductance states, AMPA receptor channel noise was low and AMPA current fluctuations tightly
32 reflected changes in the amount of glutamate released. We next showed that these two factors, channel
33 noise and fluctuations in glutamate release, were sufficient to explain the observed variability of the
34 NMDA to AMPA current ratio in quantal events recorded from the same neuron. We therefore
35 concluded that the proportion of AMPA and NMDA receptors was similar, or roughly similar, across
36 synapses onto the same target cell.

37

38 **INTRODUCTION**

39 Excitatory glutamatergic synapses in the vertebrate central nervous system (CNS) transmit via two
40 types of ligand gated ion channels, the AMPA and the NMDA receptors. These two types of receptors
41 differ by their pharmacological and biophysical properties. AMPA receptors are low affinity ligand-
42 gated channels with fast deactivation whereas NMDA receptors are high affinity receptors with
43 prolonged activation (Traynelis et al., 2010). Consequently, they have different roles. AMPA receptors
44 mainly detect fast glutamate transients whereas NMDA receptors also sense slowly changing and steady
45 state glutamate levels (Yang and Xu-Friedman, 2015). In addition, being highly permeable to calcium
46 ions, NMDA receptors play a key role in activity-induced long term changes in synaptic strength and
47 neuronal excitability. Because of these differences in role and behavior between the two receptor types,
48 the NMDA to AMPA receptor ratio is a key parameter that strongly influences the integrative properties
49 of excitatory synapses. Expression levels of AMPA and NMDA receptor subunits in post synaptic
50 membranes are highly variable and depend on the region investigated, the target neuron type and/or the
51 origin of the fibers that give rise to the presynaptic boutons (Nusser et al., 1998; Nyiri et al., 2003;
52 Shinohara et al., 2008; Tarusawa et al., 2009; Dong et al., 2010; Fukazawa and Shigemoto 2012; Rubio
53 et al., 2014). Furthermore, several forms of synaptic plasticity rely on changes in postsynaptic receptor
54 numbers, especially AMPA receptors numbers, indicating that receptor expression levels at synapses
55 may vary with time and state (Turrigiano, 2000). The factors that determine the relative abundance of
56 AMPA and NMDA receptors in a particular synapse remain largely unidentified. Several studies suggest
57 that the ratio between the two receptors is for a large part a pathway-specific property. In CA1
58 pyramidal cells for instance, responses from perforant path and Schaffer collateral synapses differ by
59 their AMPA to NMDA charge ratio (Otmakhova et al., 2002). Likewise, cortico-striatal and thalamo-
60 striatal pathways elicit responses with different NMDA/AMPA current ratios in striatal neurons (Smeal
61 et al., 2008; Ellender et al., 2013). Thalamic reticular neurons also receives two types of inputs with
62 different NMDA/AMPA current ratios (Deleuze and Huguenard, 2016). However, these data should be

63 interpreted with caution. As discussed in Myme et al (2003), synaptic responses evoked by electrical
64 stimulation of afferent pathways may fail to provide a reliable view of receptor equipment at synapses.
65 Other studies provide a different view. Recordings performed on hippocampal and neocortical neurons
66 show that the amplitudes of AMPA and NMDA receptor currents are correlated across quantal events
67 recorded from the same cell, suggesting that different synapses onto the same target neuron have a
68 relatively constant ratio of each receptor type (Gompert et al., 1998 ; Umemiya et al., . 1999; Watt et al.,
69 2000; Myme et al., 2003; Watt et al., 2004).

70 The aim of the present study was to determine whether AMPA to NMDA receptor ratio is similar or
71 varies across synapses onto the same neuron. We investigated this question by analyzing the sources of
72 current fluctuations across quantal synaptic responses recorded from a single neuron. Our main
73 objective was to determine whether current ratio variability was high, suggesting heterogeneity of
74 synapses as regards receptor ratio, or low enough to be fully explainable by stochastic factors known to
75 induce current fluctuations at a single synapse (channel noise, variations in vesicular transmitter
76 content). Recording of miniature excitatory post-synaptic currents (mEPSCs) were obtained from
77 retrogradely-identified output neurons of the nucleus tractus solitarii (NTS), a brainstem sensory relay
78 nucleus which receives glutamatergic inputs from visceral afferent fibers via the glossopharyngeal and
79 the vagus nerves and in turn projects onto various brain regions (see Baude et al., 2009 for review). The
80 contribution of stochastic factors to AMPA and NMDA current variability was estimated both by a
81 theoretical approach based on the binomial law and by computer simulations performed using a
82 stochastic synapse model.

83 **METHODS**

84 Experiments were performed on young (3-6 weeks old) male Wistar rats. All procedures were in
85 agreement with the European Communities Council directive (86/609/EEC).

86 *Electrophysiological recordings*

87 Recordings were obtained from NTS projections neurons identified by retrograde tracing (Strube et al.,
88 2015). Briefly, young adult rats were anesthetized by an intraperitoneal injection of a mixture of
89 ketamine (50 mg/kg, Imalgène 1000, Centravet, Lapalisse, France) and xylazine (15 mg/kg, Rompun

90 2%, Centravet) and placed in a stereotaxic apparatus with the incisor bar 2 mm below horizontal.
91 Tracing was performed using either red RetroBeads (undiluted Rhodamine-labeled latex microspheres,
92 Lumafluor Inc., Naples, FL, USA) or Fluorogold (2% in 0.2% saline, Fluorochrome LLC., Denver, CO,
93 USA). Tracer (100 nl) was pressure-delivered through a Hamilton syringe connected to a stainless
94 needle (ID: 0.15 mm, OD: 0.25 mm) at a rate of 1 nl s⁻¹ in the parabrachial nucleus (PBN) or the
95 caudal ventrolateral medulla (CVLM). After wound closure and recovery from anaesthesia, the animals
96 were housed individually. Preparation of medullary slices was made as described before (Balland et al.,
97 2006, 2008; Strube et al., 2015) four to seven days after retrograde tracer injection. For recordings,
98 slices were perfused in a chamber at around 3 ml/min with oxygenated ACSF containing (in mM) 120
99 NaCl, 3 KCl, 26 NaHCO₃, 1.25 KH₂PO₄, 0.5 ascorbate, 2 pyruvate, 3 myoinositol, 10 glucose, 2.5
100 CaCl₂, 2.5 MgCl₂, 0.02 D-serine and a mixture of GABA_A receptors blockers (in μM: 20 bicuculline,
101 100 picrotoxin) at 32°C. Labeled neurons were visualized using a upright microscope (BX51WI,
102 Olympus Corp., Tokyo, Japan) equipped for fluorescence detection. Whole-cell patch-clamp of NTS
103 neurons were made with an Axopatch 200B (Axon instruments, Foster city, CA, USA), filtered at 2
104 kHz and digitized at 20 kHz. Series resistance was monitored throughout the experiment and neurons in
105 which this parameter was > 20 MΩ or not stable were discarded. Patch electrodes (2-4 MΩ) contained
106 in mM: 120 cesium methane sulfonate, 10 NaCl, 1 MgCl₂, 1 CaCl₂, 10 EGTA, 2 ATP, 0.3 GTP, 10
107 Glucose, 10 HEPES (pH 7.4). Recordings were performed at +40 mV in order to remove NMDA
108 receptor magnesium block. To record mEPSCs, 1 μM TTX was added to the external solution. A
109 computer interfaced to a 12-bit A/D converter (Digidata 1200 using Clampex 9.x; Molecular Devices
110 LLC, Sunnyvale, CA, USA) controlled the voltage clamp protocols and data acquisition.

111 ***Data analysis***

112 Detection of mEPSCs was carried out using the event detection module from the Clampfit software
113 (pClamp, Molecular Device). To prevent any loss of data, detection was performed with two templates,
114 corresponding to events with high or low NMDA/AMPA current ratio respectively, using a loose
115 template match stringency (threshold set to 4). False positives were removed by visual examination of
116 each putative event. A minimum of 30 mEPSCs were collected per neuron. AMPA current amplitude
117 (I_{AMPA}) was measured at the peak of the mEPSC (current averaged over 0.3 ms). NMDA current

118 amplitude (I_{NMDA}) was obtained by averaging current within a time window starting 5 ms after onset.
119 We used 5ms duration time windows (as in Watt et al 2000, Hanse and Gustafsson 2001, Myme et al.
120 2003) since long averaging periods (50 ms) resulted in very high dispersion of data. Measures of
121 variability for I_{AMPA} , I_{NMDA} and $I_{\text{NMDA}}/I_{\text{NMDA}}$ ratio were obtained by calculating variances (σ) and/or
122 coefficients of variation (CVs). CVs were used when dimensionless comparison was required.
123 Statistical analysis were performed using the Graphpad Instat software.

124 ***Computer simulation***

125 Simulation was performed using a Monte-Carlo model of a glutamatergic synapse (Kessler, 2013). The
126 radii of the axon-dendrite apposition and of the active zone-PSD interface were 500 nm and 200 nm,
127 respectively. No glial membrane or glutamate transporter was included in the model. Glutamate was
128 released in front of PSD center. Depending on the experiment, the number of glutamate molecules
129 released at each synaptic event was either set to 3000 or made variable around a 3000 average value
130 using a Gaussian random number generator. Quantum size was limited by low and high cut-offs set at
131 1000 and 9000 molecules respectively. Glutamate diffusion was calculated using the equation for
132 Brownian displacement in a three dimensional space:

$$133 \quad \langle r^2 \rangle = 6Dt$$

134 The elementary time step t was set to 10 ns and the coefficient of diffusion for glutamate D was set to
135 $0.4 \mu\text{m}^2.\text{ms}^{-1}$. AMPA and NMDA receptors were randomly placed in the PSD. NMDA receptors were a
136 mix of GluN2A- and GluN2B-containing receptors (2:8 ratio) to comply with the known presence of
137 GluN2B subunits in NTS NMDA receptors (Zhao et al., 2015). AMPA receptor activation was
138 calculated using the kinetic scheme and rate constants for GluA2-containing receptors from Robert et
139 al. (2005). NMDA receptor activation was calculated using the kinetic scheme 4 from Erreger et al.
140 (2005) and temperature-adjusted rate constants from Santucci and Raghavachari (2008). Temperature
141 correction of NMDA receptor rates was necessary to get rise and decay phases matching those obtained
142 in recording experiments in order to perform measurements in similar conditions. Binding probabilities
143 (P_{on}) were calculated from association rate constants (k_{on}) using the following formula:

144
$$P_{on} = \frac{k_{on} dt}{0.5 N_A A_T \sqrt{2 D dt}}$$

145 where N_A is the Avogadro number, A_T is the receptor surface area set to 100 nm² and D is the diffusion
146 coefficient for glutamate in water (see Kessler 3013, for details). The receptor surface area A_T was used
147 to calculate both collisions of glutamate molecules with receptors and binding probabilities. Thus, it
148 exact value had no incidence on the output of the simulation provided that it was set below an upper
149 limit given by the inverse of the receptor density. The accuracy of binding probability calculation was
150 verified by comparing association curves (without dissociation) obtained by Monte-Carlo methods with
151 those obtained by solving ordinary differential equations using a very simple model consisting in a
152 finite disk (500 nm radius, 12 nm height) populated with 1000 binding sites and 8000 homogeneously
153 dispersed glutamate molecules. Unbinding and transition rates were converted to probabilities using the
154 following general formula :

155
$$P_i = k_i dt$$

156 For receptor current calculation, transmembrane potential was set to +40 mV. AMPA receptor
157 conductance was set to 7, 14 and 20 pS for the di-, tri- and quadri-liganded states, respectively. NMDA
158 receptor conductance was set to 50 pS. I_{AMPA} was measured at the peak of the response. Depending on
159 the experiment, I_{NMDA} was either measured 5 ms after glutamate release or obtained by averaging
160 current within a 5 ms duration time window (from 5 to 10 ms after release) in order to match
161 measurements performed on recorded mEPSCs.

162 **RESULTS**

163 *Variability in mean I_{NMDA}/I_{AMPA} ratio across NTS neurons.*

164 Recordings were obtained from a total sample of 43 NTS output neurons (see example in Fig. 1A),
165 among which 20 sent projections to PBN and 23 to the CVLM. Data from the two groups of neurons
166 were pooled after checking that there was no significant difference in main mEPSC characteristics
167 according to the projection site (PBN vs CVLM). The frequency of mEPSCs was highly variable
168 ranging from 0.1 to 1 Hz, depending on the neuron (median : 0.22 Hz). At +40 mV, most individual

169 mEPSCs were composite mEPSCs with both a fast and a slow component attributable to AMPA and
170 NMDA receptor activation (I_{AMPA} and I_{NMDA}), respectively (Aylwin et al 1997; Balland et al, 2006, 2008,
171 Zhao et al. 2015). We verified that the slow component was suppressed by APV and thus entirely due to
172 NMDA receptor activation (Fig. 1A). Mean I_{AMPA} (μ_{AMPA}) exhibited little variability between cells.
173 Depending on the neuron, it ranged from 14 to 27 pA. On the contrary, mean I_{NMDA} (μ_{NMDA}) exhibited
174 five-fold variation across neurons, ranging from 2 to 10 pA. As a consequence, mean I_{NMDA}/I_{AMPA} ratio
175 (μ_{RATIO}) was also highly variable across neurons, ranging from 0.12 to 0.49 (Fig 1B).

176 ***Variability in quantal events recorded from the same NTS neuron. Fluctuations of I_{NMDA}/I_{AMPA} ratio***
177 ***mainly result from variations of I_{NMDA}***

178 To compare the variabilities of I_{NMDA} , I_{AMPA} and I_{NMDA}/I_{AMPA} ratio across mEPSCs recorded from the same
179 cell we calculated their respective CVs. Intra-neuronal I_{NMDA}/I_{AMPA} ratio variability was in some cases
180 relatively high with CV_{RATIO} values up to 0.94 (range 0.22-0.94, depending on the neuron ; Fig 1C). We
181 wondered whether this was due to fluctuations in I_{AMPA} , or I_{NMDA} or both. Whatever the neuron, $CV_{I_{AMPA}}$
182 was low ranging from 0.17 to 0.40, indicating little fluctuation from one quantal event to the other (Fig.
183 1C). I_{NMDA} was far more variable with $CV_{I_{NMDA}}$ being up to 0.93 and less than 0.4 for 1 neuron only (Fig.
184 1C). We concluded that fluctuations in I_{NMDA}/I_{AMPA} ratio across mEPSCs recorded from the same cell
185 originated from variations in I_{NMDA} rather than variations in I_{AMPA} . This finding was confirmed by
186 regression analysis (coefficients of determination : 0.79 versus 0.02, respectively; see Fig. 1D,E). We
187 wondered whether high intra-neuronal variability of I_{NMDA} as compared to I_{AMPA} resulted from
188 differences in receptor channel properties or from stronger variations in NMDA than AMPA receptor
189 content across synapses from the same target cell. To answer this question, we tried to estimate the
190 contribution of stochastic factors to I_{NMDA} and I_{AMPA} variabilities.

191 ***Stochastic factors of I_{NMDA} variability***

192 Two main stochastic factors may contribute to receptor current variability across mEPSCs: random
193 transitions between receptor channel closed and open states (channel noise) and fluctuations in quantal
194 glutamate release. To estimate I_{NMDA} variability resulting from random receptor channel closing and
195 opening, we first calculated channel noise variance according to the binomial distribution. Indeed, if
196 variations of I_{NMDA} across mEPSCs were exclusively due to this factor (i.e. no variation in receptor

197 number, no variation in neurotransmitter quantum size, instantaneous equilibrium of glutamate
198 concentrations within the cleft), then I_{NMDA} would follow a binomial distribution and the resulting
199 variance σ^2_{CN} should be equal to (Sigworth, 1980 ; Robinson et al., 1991):

$$200 \quad \sigma^2_{\text{CN}} = i \cdot \mu_{\text{INMDA}} - \frac{\mu_{\text{INMDA}}^2}{N} \quad (1)$$

201 where N is the number of NMDA receptors and i the unitary receptor current. Since I_{NMDA} is the product
202 of the unitary receptor current i by the number of open channels NP_{op} (P_{op} being the average open
203 probability of NMDA receptors in the synapse), equation 1 may be linearized as follows:

$$204 \quad \sigma^2_{\text{CN}} = \mu_{\text{INMDA}} [i(1 - P_{op})] \quad (2)$$

205 In our experiments, the driving force was set + 40 mV. Thus, i was estimated to be about 2 pA (50 pS
206 unitary conductance for GluN2B-containing NMDA receptors, see Traynelis et al., 2010). Assuming a
207 realistic P_{op} value of 0.1 (Kessler, 2013), we compared I_{NMDA} variances (σ^2_{INMDA}) obtained from recorded
208 neurons with the σ^2_{CN} curve calculated from equation 2 (Fig. 2A). It should be kept in mind that σ^2_{INMDA}
209 values are likely to have been underestimated since averaging I_{NMDA} measurements over 5 ms duration
210 time-window may have resulted in some smoothing of inter-event fluctuations (see methods).
211 Nevertheless, this comparison suggests that a large part of I_{NMDA} variability across mEPSCS was
212 accounted for by channel noise.

213 Equation 1 relies on the assumption that every NMDA receptor channel in a synapse has the same P_{op} .
214 This may not be the case since glutamate concentrations decline with distance to the release site. We
215 thus tried to obtain estimates of σ^2_{CN} that take into account possible differences in P_{op} between receptors
216 according to their location relative to the release site. This was done by computer simulation using a
217 Monte Carlo model of a glutamatergic synapse. Simulation was performed in 10 series of 50 runs each,
218 each run representing a different quantal event. The amount of glutamate released was held constant
219 (3000 molecules) throughout runs and series. The number of NMDA receptors in the synapse was
220 adjusted between series (from 10 to 100) in order to span the entire range of mean I_{NMDA} values obtained
221 from recorded neurons. I_{NMDA} values were measured 5 ms after onset. We compared σ^2_{INMDA} obtained by
222 simulation with the σ^2_{CN} curve calculated from equation 2 using the average P_{op} value of NMDA

223 receptors in simulated data (0.07). The fit between the theoretical curve and the simulated data was
224 nearly perfect (Fig. 2B) indicating that binomial distribution based on an averaged P_{op} provides an
225 accurate description of the stochastic behavior of synaptic NMDA receptors.

226 We next used computer simulation to get estimate of I_{NMDA} variability resulting from fluctuations in
227 glutamate release. Simulation was performed using a randomly determined amount of glutamate
228 released for each run (see methods). The within-series average was close to 3000 glutamate molecules
229 with either a low (CV_{Glu} ranging from 0.26 to 0.31, depending on the series) or a high (CV_{Glu} ranging
230 from 0.50 to 0.62, depending on the series) variability. Surprisingly, we found little difference between
231 σ^2_{NMDA} values obtained using either a constant or a randomly varying amount of glutamate release (Fig.
232 2C,D) suggesting that the part of I_{NMDA} variability resulting from release fluctuations is small as
233 compared to that resulting from channel noise. This finding may seem at odds with the current view
234 which states that channel noise minimally contribute to quantal current variability. This view was
235 mainly based on studies dealing with I_{AMPA} variability (see for instance Franks et al., 2002 ; 2003). We
236 therefore compared the stochastic behavior of AMPA and NMDA receptors placed in identical
237 conditions.

238 ***Comparison between I_{NMDA} and I_{AMPA} stochastic behavior***

239 Simulation was performed with 100 NMDA receptors and 100 AMPA receptors in the PSD. A first
240 series was obtained with a constant amount of glutamate release throughout runs. Subsequent series
241 were obtained with randomly determined numbers of glutamate molecules released (series average \approx
242 3000), using parameters adjusted in order to obtain low, moderate or high release variability (CV_{Glu} : 0.3,
243 0.54 and 0.62, respectively). To allow comparison between I_{NMDA} and I_{AMPA} , variances were converted
244 into CVs. We found that contrary to CV_{NMDA} , $CV_{I_{AMPA}}$ was very low using constant release and steeply
245 increased with CV_{Glu} (Fig. 3A,B). Plotting individual currents values within a series against the amount
246 of glutamate released illustrated the different behaviors of the two receptors (Fig. 3C,D). While I_{AMPA}
247 amplitudes were strongly correlated with release (coefficient of determination : 0.77), I_{NMDA} amplitudes
248 were only loosely correlated with glutamate molecules numbers (coefficient of determination : 0.21). A
249 first factor that may explain this difference is the fact that AMPA receptors had an higher average open
250 probability than NMDA receptors. In addition, AMPA receptors have subconductance states that depend

251 on the number of bound glutamate molecules (Traynelis et al. 2010). It should be kept in mind that
 252 equation 2 derives from the binomial distribution and applies to channels that exist in conducting and
 253 non-conducting states only, a more complex mathematical description being required for channels with
 254 subconductance states, (see Neher and Stevens, 1977). Accordingly, we showed that removing the
 255 partially-conducting states (i.e., the di and tri-liganded states) in the AMPA receptor scheme increased
 256 I_{AMPA} variability to levels expected from equation 2, indicating that the presence of subconductance
 257 states decreases channel noise (Fig. 3E). Noise reduction by subconductance states was substantial as
 258 shown by the two-third decrease in variance. Taken as a whole these data point out the fact that,
 259 contrary to I_{NMDA} variability which mainly results from receptor noise, I_{AMPA} variability at a single
 260 synapse tightly reflects fluctuations in glutamate release. These differences between AMPA and NMDA
 261 receptor behaviors may have contributed to the variability of the I_{NMDA}/I_{AMPA} ratio across mEPSCs
 262 recorded from the same cell.

263 *The origin of of I_{NMDA}/I_{AMPA} ratio variability in quantal events recorded from NTS neuron*

264 We next wondered what would be I_{NMDA}/I_{AMPA} ratio variability if there were no difference in
 265 NMDA/AMPA receptor proportions between synapses onto the same target cell. We estimated σ^2_{Ratio} by
 266 using first the order Taylor expansion (van Kempen and van Vliet, 2000):

$$267 \quad \sigma^2_{Ratio} \approx \frac{\mu_{INMDA}^2}{\mu_{IAMPA}^2} \left[\frac{\sigma_{INMDA}^2}{\mu_{INMDA}^2} + \frac{\sigma_{IAMPA}^2}{\mu_{IAMPA}^2} - \frac{2\rho_{(INMDA, IAMPA)}\sigma_{INMDA}\sigma_{IAMPA}}{\mu_{NMDA}\mu_{IAMPA}} \right] \quad (3)$$

268 where $\rho_{(INMDA, IAMPA)}$ is the correlation coefficient between I_{NMDA} and I_{AMPA} . Since I_{NMDA}/I_{AMPA} ratio
 269 variability was primarily due to variations in I_{NMDA} (see Fig. 1E), we reasoned that receptor ratio
 270 heterogeneity across synapses, if present, would primarily result in increased I_{NMDA} fluctuation. Thus, to
 271 eliminate potential effects of synapses heterogeneity, we replaced σ^2_{INMDA} and σ_{INMDA} in equation 3 by σ
 272 $^2_{CN}$ and σ_{CN} values obtained from equation 2 :

$$273 \quad \sigma^2_{Ratio} \approx \frac{\mu_{INMDA}^2}{\mu_{IAMPA}^2} \left[\frac{i(1-P_{op})}{\mu_{INMDA}} + \frac{\sigma_{IAMPA}^2}{\mu_{IAMPA}^2} - \frac{2\sqrt{i(1-P_{op})}\rho_{(INMDA, IAMPA)}\sigma_{IAMPA}}{\sqrt{\mu_{NMDA}\mu_{IAMPA}}} \right] \quad (4)$$

274 Calculation was performed for each neuron using the experimentally obtained values for μ_{INMDA} , μ_{IAMPA} ,
 275 σ^2_{IAMPA} and $\rho_{(INMDA, IAMPA)}$. Comparing σ^2_{Ratio} values directly obtained from recorded data and those

275 recalculated from equation 4 showed that the observed $I_{\text{NMDA}}/I_{\text{AMPA}}$ ratio variability was largely
276 attributable to stochastic factors (Fig. 4A,B). Especially, the slope of the regression line of recorded
277 values on calculated values was close to 1 (Fig. 4B) indicating that experimentally observed variability
278 was on average close to that expected if I_{NMDA} fluctuations were entirely due to channel noise.

279 To confirm this finding, we performed simulation according to two scenarios, one assuming that the
280 ratio of NMDA to AMPA receptors at synapses varies between neurons but is strictly identical across
281 the different synapses onto the same neuron (scenario 1, Fig. 4C), the other assuming that the relative
282 abundance of AMPA and NMDA receptors at synapses depends on the afferent pathway only and thus
283 differs between synapses onto the same target cell (scenario 2, Fig 4E). Each neuron was simulated by a
284 series of 50 runs, each run representing a quantal event occurring at a different synapse. The numbers of
285 AMPA and NMDA receptors in the simulation were adjusted in order to fit the averaged quantal
286 currents recorded in actual NTS neurons. We kept the AMPA receptor number constant (100 per
287 synapse) across simulated neurons and we adjusted the overall number of NMDA receptors neuron by
288 neuron in order to span the entire range of μ_{INMDA} values found in recorded cells. Release variability was
289 adjusted ($CV_{\text{Glu}} \approx 0.3$) in order to obtain $\sigma^2_{I_{\text{AMPA}}}$ close to those calculated for recorded neurons. I_{NMDA}
290 value was obtained by averaging current over a 5 ms time windows (see methods).

291 We then plotted σ^2_{Ratio} values obtained from either recorded or simulated neurons against μ_{INMDA} .
292 Variances measured from recorded mEPSCs were very close to values provided by simulation using
293 scenario 1 (Fig. 4D) and far below those obtained using scenario 2 (Fig. 4F), confirming that the
294 variability of the $I_{\text{NMDA}}/I_{\text{AMPA}}$ ratio found in mEPSCs recorded from the same cell resulted from channel
295 noise and fluctuations in glutamate release rather than from heterogeneity of receptor ratio across
296 synapses.

297 ***Correlation between I_{NMDA} and I_{AMPA} across mEPSCs from the same neuron***

298 We wondered whether a similar NMDA to AMPA receptor ratio across a neuron's synapses would
299 invariably result in a strong correlation between I_{NMDA} and I_{AMPA} in mEPSCs. Even with fully-identical
300 receptor ratio, one may expect the correlation to vanish if NMDA channel noise is high enough. Signal
301 to noise ratio (SNR) calculated from the binomial distribution is equal to:

302
$$SNR = \sqrt{\frac{N \cdot P_{op}}{[(1 - P_{op})]}}$$

303 We reasoned that, since SNR increases with the square root of the receptor number N , the strength of
304 the correlation between I_{NMDA} and I_{AMPA} should likewise increase with NMDA receptor number. We first
305 look at quantal events simulated using scenario 1. We found a significant correlation between I_{NMDA} and
306 I_{AMPA} for most but not all simulated neurons. Furthermore, the strength of the correlation was highly
307 variable (see examples in Fig. 5A). For the 27 neurons simulated using scenario 1, Pearson r
308 coefficients ranged from 0.14 to 0.65. As expected, correlation strength was found to linearly increase
309 with receptor number in synapses (the only changing parameter between neurons in scenario 1) and
310 hence with μ_{INMDA} (Fig. 5B). We next examined recorded neurons. Most but not all (34 out of 43)
311 exhibited significant correlation between I_{NMDA} and I_{AMPA} (see example in Fig 5C). Pearson r coefficients
312 ranged from 0.27 to 0.89 and increased with μ_{INMDA} (Fig 5D), consistent with the view that loose or
313 lacking correlation resulted from high relative NMDA channel noise rather than synapses heterogeneity.

314 **DISCUSSION**

315 Here we found that quantal events recorded from the same NTS projection neuron exhibited substantial
316 variations in I_{NMDA}/I_{AMPA} ratio. Using both a theoretical approach and numerical simulation, we showed
317 that variability of I_{NMDA}/I_{AMPA} ratio was mostly if not entirely explainable by two factors: i) channel noise
318 being especially strong at NMDA receptors, and ii) fluctuations in glutamate release having stronger
319 effects on I_{AMPA} than on I_{NMDA} . These findings rule out any substantial contribution of synapse
320 heterogeneity to the variability of I_{NMDA}/I_{AMPA} ratio. They therefore imply that the proportions of AMPA
321 and NMDA receptors was similar, or roughly similar, across synapses onto the same target cell. In
322 addition, we found strong differences in mean I_{NMDA}/I_{AMPA} ratio between neurons. Thus, our results
323 support the idea that the receptor ratio in synapses is determined by the target cell rather than the
324 afferent pathway. This conclusion is reminiscent of previous findings showing that different synapses
325 onto the same neocortical neuron have very similar NMDA to AMPA receptor ratios (Umekiya et al.,
326 1999; Watt et al., 2000; Myme et al., 2003; Watt et al., 2004) and raises the question of whether
327 mechanisms exist that co-regulate AMPA and NMDA receptor expression in postsynaptic membranes.

328 As yet, AMPA and NMDA receptor trafficking are viewed as independent processes. To the best of our
329 knowledge, there is no evidence for co-transport of AMPA and NMDA receptors through secretory or
330 endosomal recycling pathways. Likewise, there is no data suggesting that AMPA and NMDA
331 insertion/stabilization in postsynaptic membrane are tightly linked to each other. Alternatively, a
332 conserved receptor ratio across synapses may be the passive consequence of structural constraints.
333 Electron microscope studies performed in various CNS regions using either post-embedding
334 immunogold labeling, freeze fracture replica immunolabeling or STEM tomography indicate that the
335 number of AMPA receptors in synaptic clusters linearly scales with PSD size (Takumi et al., 1999;
336 Racca et al., 2000; Tanaka et al., 2005; Masugi-Tokita et al., 2007; Antal et al., 2008; Shinohara et al.,
337 2008; Dong et al., 2010; Rubio et al., 2014; Chen et al., 2015). NMDA receptor number in synaptic
338 clusters also correlates with PSD size in several brain areas (Racca et al., 2000; Nyiri et al., 2003;
339 Tarusawa et al., 2009; Rubio et al., 2014; but see Takumi et al., 1999; Shinohara et al., 2008; Chen et
340 al., 2015). Thus, it may be hypothesized that the postsynaptic membrane includes finite numbers of
341 specific potential slots for AMPA and NMDA receptors and that the number of slots for each receptor
342 linearly scales with the PSD area. The slot hypothesis was originally proposed to explain how synapses
343 acquire additional AMPA receptors during postsynaptic LTP (Shi et al., 2001; see also Lisman and
344 Raghavachari, 2006; Opazo et al., 2012). It was also postulated that potential slots are not always fully
345 filled with receptors. In this context, a possible interpretation for our data is that the degree of filling of
346 potential NMDA slots is similar across a NTS neuron's synapses but differs between NTS neurons,
347 presumably because of differences in readily available extrasynaptic receptors pools.

348 An unexpected finding from our simulation experiments was the fact that I_{NMDA} and I_{AMPA} fluctuations
349 across mEPSCs originated from different sources. I_{NMDA} variability was mainly postsynaptic as it
350 resulted from strong channel noise overwhelming the influence of release variations. On the contrary,
351 AMPA receptor channel noise was low and I_{AMPA} variability was mainly presynaptic, tightly reflecting
352 variations in the amount of glutamate released. The lower variability of I_{AMPA} as compared to I_{NMDA} as
353 observed in the present study both *in vivo* and *in silico* is in line with previous results obtained by
354 single synapse recording on hippocampal cell cultures (McAllister and Stevens, 2000). Data in Table 1
355 from McAllister and Stevens (2000) indicate that the CV of the AMPA component across responses

356 from a single synapse ranged between 0.27 and 0.43, depending on the synapse, while the CV of the
357 NMDA component across the same responses ranged between 0.56 and 0.82, depending on the synapse.
358 It has been claimed previously that differences between the variability of AMPAR and NMDAR
359 responses were due solely to unequal numbers of receptors at the synapse (Franck et al., 2002 ; 2003).
360 This claim was based on simulations performed with simplified kinetic schemes including few receptor
361 states (Lester and Jahr, 1992 for NMDA receptors and Jonas et al, 1993 for AMPA receptors). Here,
362 using recently published more realistic Markov models (Roberts et al, 2005 for AMPA receptors and
363 Erreger et al. 2005 for NMDA receptors), we unraveled an unexpected biophysical difference between
364 the two receptors. We found that the intrinsic noise of AMPA channels is lower than that of NMDA
365 channels partly as a consequence of AMPA receptors having subconductance states. In addition, the
366 gradual opening of the AMPA receptor pore with the number of bound glutamate molecules provides a
367 mechanism by which unitary receptor current increases with cleft glutamate concentration. In conclusion,
368 our data show that AMPA receptors are endowed with specific features that reduce the variability of the
369 early as compare to the late NMDA receptor-dependent phase of the postsynaptic response. From a
370 functional point of view, these AMPA receptor specific features may fulfill an important role by
371 increasing the temporal precision and the reliability of fast excitatory transmission.

372

373 Acknowledgments. We wish to thank Dr Lydia Kerkerian and Dr Francis Castets for their helpful
374 comments on the manuscript. We also express our gratitude to Dr Boris Barbour for judicious advice in
375 early steps of the study.

376 **References**

- 377 Antal M, Fukazawa Y, Eördögh M, Muszil D, Molnár E, Itakura M, Takahashi M, Shigemoto R (2008)
378 Numbers, densities, and colocalization of AMPA- and NMDA-type glutamate receptors at individual
379 synapses in the superficial spinal dorsal horn of rats. *J Neurosci* 28:9692-96701.
- 380 Aylwin ML, Horowitz JM, Bonham AC (1997) NMDA receptors contribute to primary visceral afferent
381 transmission in the nucleus of the solitary tract. *J Neurophysiol* May;77(5):2539-2548.
- 382 Balland B, Lachamp P, Strube C, Kessler JP, Tell F (2006) Glutamatergic synapses in the rat nucleus
383 tractus solitarii develop by direct insertion of calcium-impermeable AMPA receptors and without
384 activation of NMDA receptors. *J Physiol.* 574:245-261.
- 385 Balland B, Lachamp P, Kessler JP, Tell F (2008) Silent synapses in developing rat nucleus tractus
386 solitarii have AMPA receptors. *J Neurosci* 28 :4624-4634.
- 387 Baude A, Strube C, Tell F, Kessler JP (2009) Glutamatergic neurotransmission in the nucleus tractus
388 solitarii: structural and functional characteristics. *J Chem Neuroanat* 38:145-153.
- 389 Chen X, Levy JM, Hou A, Winters C, Azzam R, Sousa AA, Leapman RD, Nicoll RA, Reese TS (2015)
390 PSD-95 family MAGUKs are essential for anchoring AMPA and NMDA receptor complexes at the
391 postsynaptic density. *Proc Natl Acad Sci U S A* 112:E6983-6992.
- 392 Deleuze C, Huguenard JR (2016) Two classes of excitatory synaptic responses in rat thalamic reticular
393 neurons. *J Neurophysiol.*116:995-1011.
- 394 Dong YL, Fukazawa Y, Wang W, Kamasawa N, Shigemoto R (2010) Differential postsynaptic
395 compartments in the laterocapsular division of the central nucleus of amygdala for afferents from the
396 parabrachial nucleus and the basolateral nucleus in the rat. *J Comp Neurol* 518:4771-91.
- 397 Ellender TJ, Harwood J, Kosillo P, Capogna M, Bolam JP (2013) Heterogeneous properties of central
398 lateral and parafascicular thalamic synapses in the striatum. *J Physiol* 591:257-72.

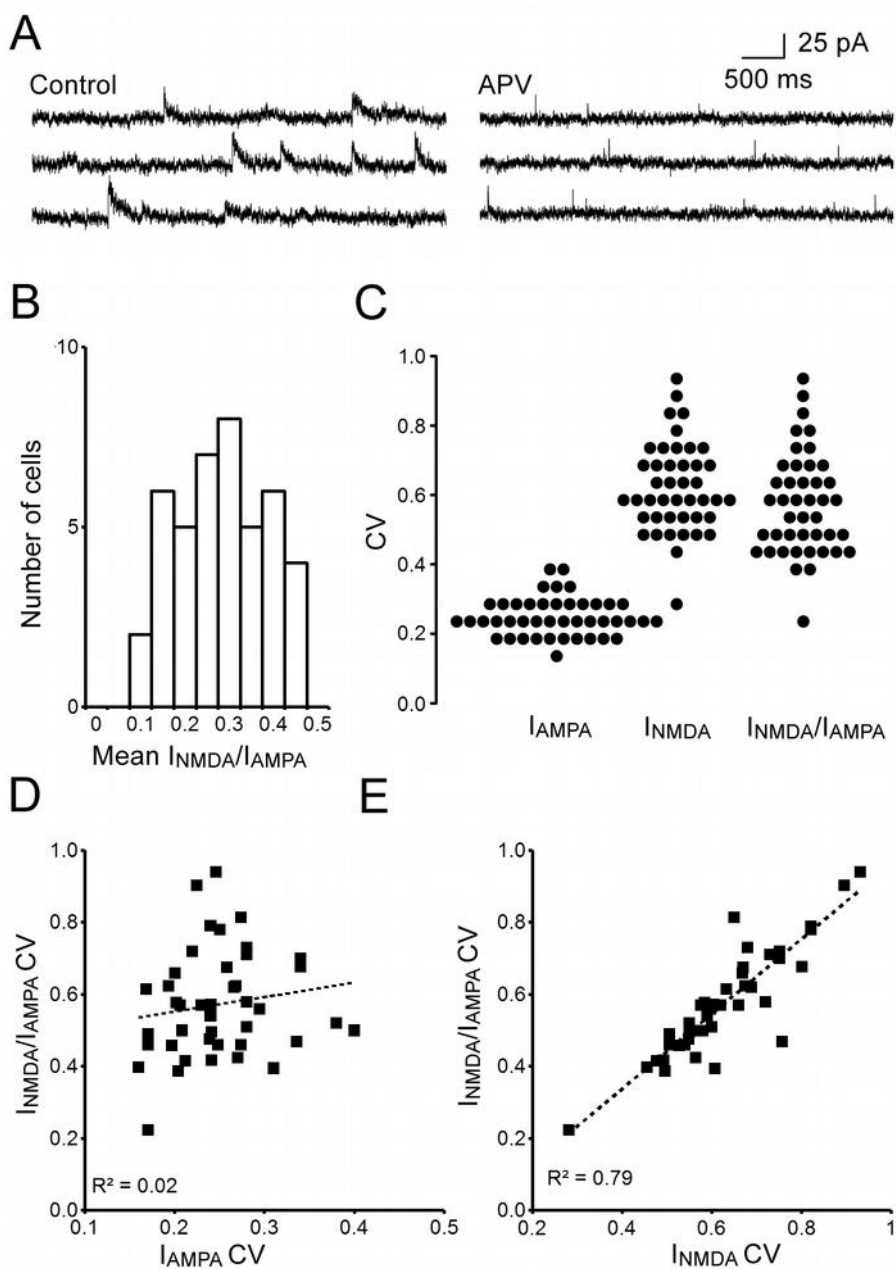
- 399 Erreger K, Dravid SM, Banke TG, Wyllie DJ, Traynelis SF (2005) Subunit-specific gating controls rat
400 NR1/NR2A and NR1/NR2B NMDA channel kinetics and synaptic signalling profiles. *J Physiol*
401 563:345-358.
- 402 Franks KM, Bartol TM Jr, Sejnowski TJ (2002) A Monte Carlo model reveals independent signaling at
403 central glutamatergic synapses. *Biophys J*. 83:2333-2348.
- 404 Franks KM, Stevens CF, Sejnowski TJ (2003) Independent sources of quantal variability at single
405 glutamatergic synapses. *J Neurosci*. 23:3186-3195.
- 406 Fukazawa Y, Shigemoto R (2012) Intra-synapse-type and inter-synapse-type relationships between
407 synaptic size and AMPAR expression. *Curr Opin Neurobiol* 22:446–452.
- 408 Gomperts SN, Rao A, Craig AM, Malenka RC, Nicoll RA (1998) Postsynaptically silent synapses in
409 single neuron cultures. *Neuron* 21:1443–1451.
- 410 Hanse E, Gustafsson B (2000) Quantal variability at glutamatergic synapses in area CA1 of the rat
411 neonatal hippocampus. *J Physiol*. 531:467-480.
- 412 Jonas P, Major G, Sakmann B (1993) Quantal components of unitary EPSCs at the mossy fibre synapse
413 on CA3 pyramidal cells of rat hippocampus. *J Physiol*. 472:615-663.
- 414 Kessler JP (2013) Control of cleft glutamate concentration and glutamate spill-out by perisynaptic glia:
415 uptake and diffusion barriers. *PLoS One* 8:e70791.
- 416 Lester RA, Jahr CE (1992) NMDA channel behavior depends on agonist affinity. *J Neurosci*.
417 12:635-43.
- 418 Lisman J, Raghavachari S (2006) A unified model of the presynaptic and postsynaptic changes during
419 LTP at CA1 synapses. *Sci STKE* 356:re11.
- 420 Masugi-Tokita M, Tarusawa E, Watanabe M, Molnár E, Fujimoto K, Shigemoto R (2007) Number and
421 density of AMPA receptors in individual synapses in the rat cerebellum as revealed by SDS-digested
422 freeze-fracture replica labeling. *J Neurosci* 27:2135–2144.

- 423 McAllister AK, Stevens CF (2000). Nonsaturation of AMPA and NMDA receptors at hippocampal
424 synapses. *Proc Natl Acad Sci U S A.* 97:6173-6178.
- 425 Myme CI, Sugino K, Turrigiano GG, Nelson SB (2003) The NMDA-to-AMPA ratio at synapses onto
426 layer 2/3 pyramidal neurons is conserved across prefrontal and visual cortices. *J. Neurophysiol* 90:771–
427 779
- 428 Neher E, Stevens CF. Conductance fluctuations and ionic pores in membranes (1977) *Annu Rev*
429 *Biophys Bioeng.* 6:345-381.
- 430 Nusser Z, Lujan R, Laube G, Roberts JD, Molnar E, Somogyi P (1998) Cell type and pathway
431 dependence of synaptic AMPA receptor number and variability in the hippocampus. *Neuron* 21:545–
432 559.
- 433 Nyíri G, Stephenson FA, Freund TF, Somogyi P (2003). Large variability in synaptic N-methyl-D-
434 aspartate receptor density on interneurons and a comparison with pyramidal-cell spines in the rat
435 hippocampus. *Neuroscience* 119:347-63.
- 436 Opazo P, Sainlos M, Choquet D (2012) Regulation of AMPA receptor surface diffusion by PSD-95
437 slots. *Curr Opin Neurobiol* 22:453-460.
- 438 Otmakhova NA, Otmakhov N, Lisman JE (2002) Pathway-specific properties of AMPA and NMDA-
439 mediated transmission in CA1 hippocampal pyramidal cells. *J Neurosci* 22:1199-207.
- 440 Racca C, Stephenson FA, Streit P, Roberts JD, Somogyi P (2000) NMDA receptor content of synapses
441 in stratum radiatum of the hippocampal CA1 area. *J Neurosci* 20:2512-2522.
- 442 Robert A, Armstrong N, Gouaux JE, Howe JR (2005) AMPA receptor binding cleft mutations that alter
443 affinity, efficacy, and recovery from desensitization. *J Neurosci* 25:3752-3762.
- 444 Robinson HP, Sahara Y, Kawai N (1991) Nonstationary fluctuation analysis and direct resolution of
445 single channel currents at postsynaptic sites. *Biophys J.* 1991 59:295-304.
- 446 Rubio ME, Fukazawa Y, Kamasawa N, Clarkson C, Molnár E, Shigemoto R (2014) Target- and input-

- 447 dependent organization of AMPA and NMDA receptors in synaptic connections of the cochlear nucleus.
448 *J Comp Neurol* 522:4023-42.
- 449 Santucci DM, Raghavachari S (2008) The effects of NR2 subunit-dependent NMDA receptor kinetics
450 on synaptic transmission and CaMKII activation. *PLoS Comput Biol.* 4:e1000208.
- 451 Shi S, Hayashi Y, Esteban JA, Malinow R (2001) Subunit-specific rules governing AMPA receptor
452 trafficking to synapses in hippocampal pyramidal neurons. *Cell* 105:331–343.
- 453 Shinohara Y, Hirase H, Watanabe M, Itakura M, Takahashi M, Shigemoto R (2008) Left-right
454 asymmetry of the hippocampal synapses with differential subunit allocation of glutamate receptors.
455 *Proc Natl Acad Sci U S A.* 105:19498-19503.
- 456 Sigworth FJ (1980) The variance of sodium current fluctuations at the node of Ranvier. *J Physiol.*
457 307:97-129.
- 458 Smeal RM, Keefe KA, Wilcox KS (2008) Differences in excitatory transmission between thalamic and
459 cortical afferents to single spiny efferent neurons of rat dorsal striatum. *Eur J Neurosci* 28:2041-2052.
- 460 Strube C, Saliba L, Moubarak E, Penalba V, Martin-Eauclaire MF, Tell F, Clerc N (2015) Kv4 channels
461 underlie A-currents with highly variable inactivation time courses but homogeneous other gating
462 properties in the nucleus tractus solitarii. *Pflugers Arch* 467:789-803.
- 463 Takumi Y, Ramírez-León V, Laake P, Rinvik E, Ottersen OP (1999) Different modes of expression of
464 AMPA and NMDA receptors in hippocampal synapses. *Nat Neurosci* 2:618-24.
- 465 Tanaka J, Matsuzaki M, Tarusawa E, Momiyama A, Molnar E, Kasai H, Shigemoto R (2005) Number
466 and density of AMPA receptors in single synapses in immature cerebellum. *J Neurosci* 25:799–807.
- 467 Tarusawa E, Matsui K, Budisantoso T, Molnár E, Watanabe M, Matsui M, Fukazawa Y, Shigemoto R
468 (2009) Input-specific intrasynaptic arrangements of ionotropic glutamate receptors and their impact on
469 postsynaptic responses. *J Neurosci* 29:12896–12908.

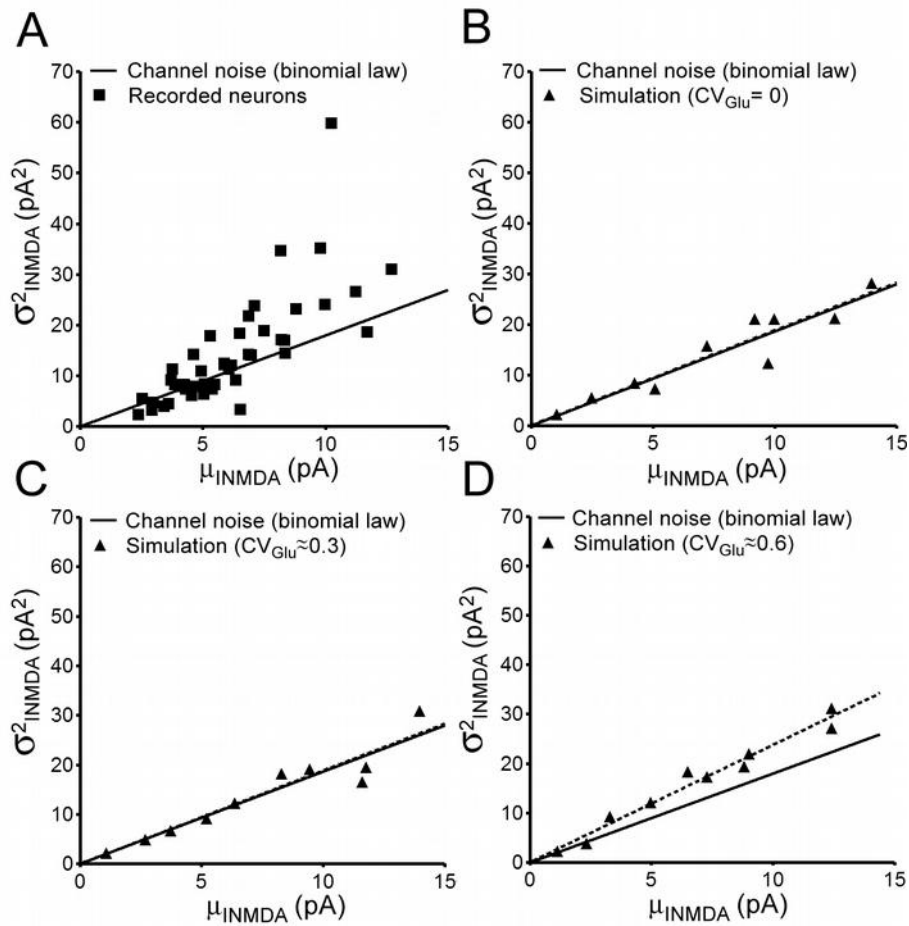
- 470 Traynelis SF, Wollmuth LP, McBain CJ, Menniti FS, Vance KM, Ogden KK, Hansen KB, Yuan H,
471 Myers SJ, Dingledine R (2010) Glutamate receptor ion channels: structure, regulation, and function.
472 *Pharmacol Rev.* 62:405-496.
- 473 Turrigiano GG (2000) AMPA receptors unbound: membrane cycling and synaptic plasticity. *Neuron.*
474 26:5-8.
- 475 Umemiya M, Senda M, and Murphy TH (1999) Behaviour of NMDA and AMPA receptor-mediated
476 miniature EPSCs at rat cortical neuron synapses identified by calcium imaging. *J Physiol* 521:113–122.
- 477 van Kempen GM, van Vliet LJ (2000) Mean and variance of ratio estimators used in fluorescence ratio
478 imaging. *Cytometry.* 39 :300-305.
- 479 Watt AJ, van Rossum MC, MacLeod KM, Nelson SB, Turrigiano GG (2000) Activity coregulates
480 quantal AMPA and NMDA currents at neocortical synapses. *Neuron* 26:659–670.
- 481 Watt AJ, Sjöström PJ, Häusser M, Nelson SB, Turrigiano GG (2004) A proportional but slower NMDA
482 potentiation follows AMPA potentiation in LTP. *Nat Neurosci.* 7:518-24.
- 483 Yang Y, Xu-Friedman MA (2015) Different pools of glutamate receptors mediate sensitivity to ambient
484 glutamate in the cochlear nucleus. *J Neurophysiol* 113:3634-3645.2015
- 485 Zhao H, Peters JH, Zhu M, Page SJ, Ritter RC, Appleyard SM (2015) Frequency-dependent facilitation
486 of synaptic throughput via postsynaptic NMDA receptors in the nucleus of the solitary tract. *J Physiol* ;
487 593:111-125.

488 **Figure Legends**

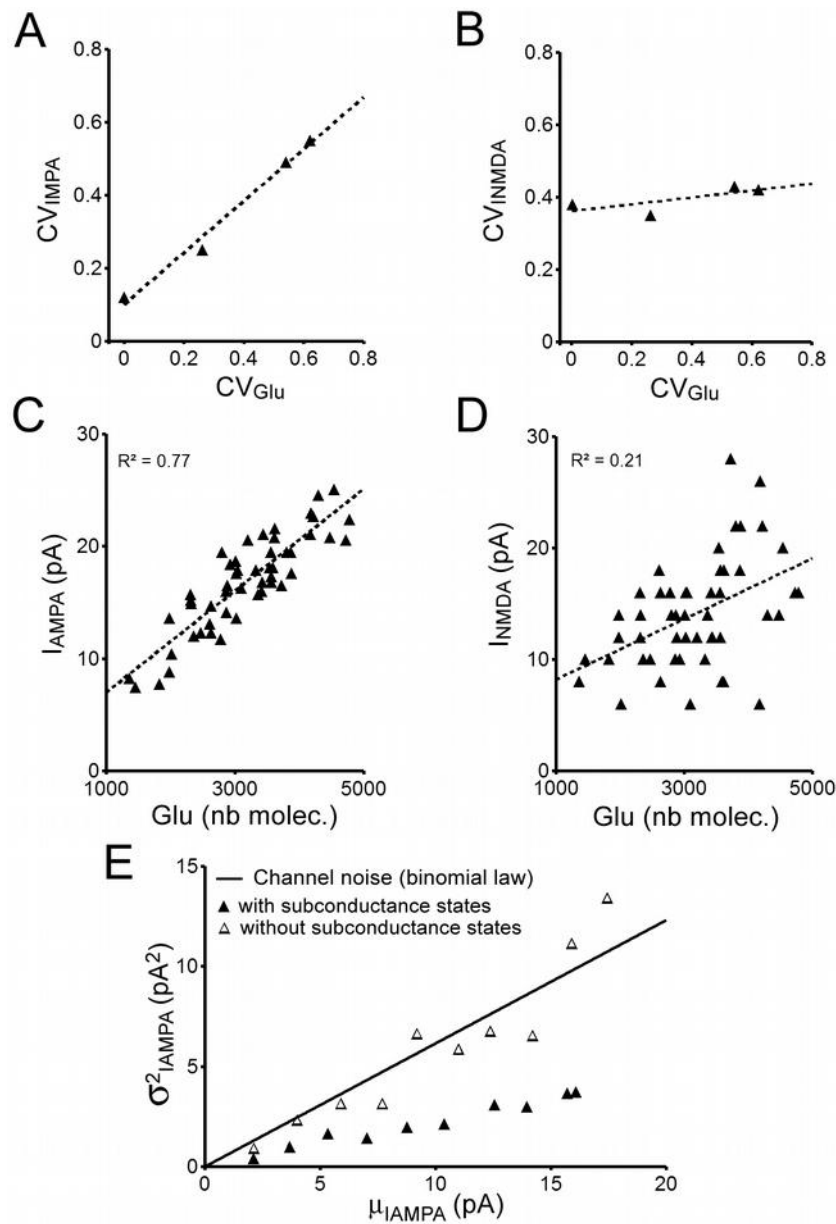


489 **Figure 1. A.** Example of recordings obtained from an NTS neuron (holding potential + 40mV). The
490 slow component of composites mEPSC recorded in control conditions is no longer present when D,L-
491 APV is added to perfusion medium (100 μ M) indicating that it is entirely due to NMDA receptors. **B.**
492 Distribution histogram of mean I_{NMDA}/I_{AMPA} ratios (μ_{RATIO}) in mEPSCs from recorded neurons (n=43). **C.**

493 Distribution histograms of I_{AMPA} , I_{NMDA} and $I_{\text{NMDA}}/I_{\text{AMPA}}$ ratio coefficients of variation (CV) in mEPSCs
494 from recorded neurons. **D.** Lack of correlation between I_{AMPA} and $I_{\text{NMDA}}/I_{\text{AMPA}}$ ratio CVs across recorded
495 neurons. **E.** $I_{\text{NMDA}}/I_{\text{AMPA}}$ ratio CV in mEPSCs from recorded neurons linearly increases with I_{NMDA} CV
496 (R^2 : coefficient of determination).

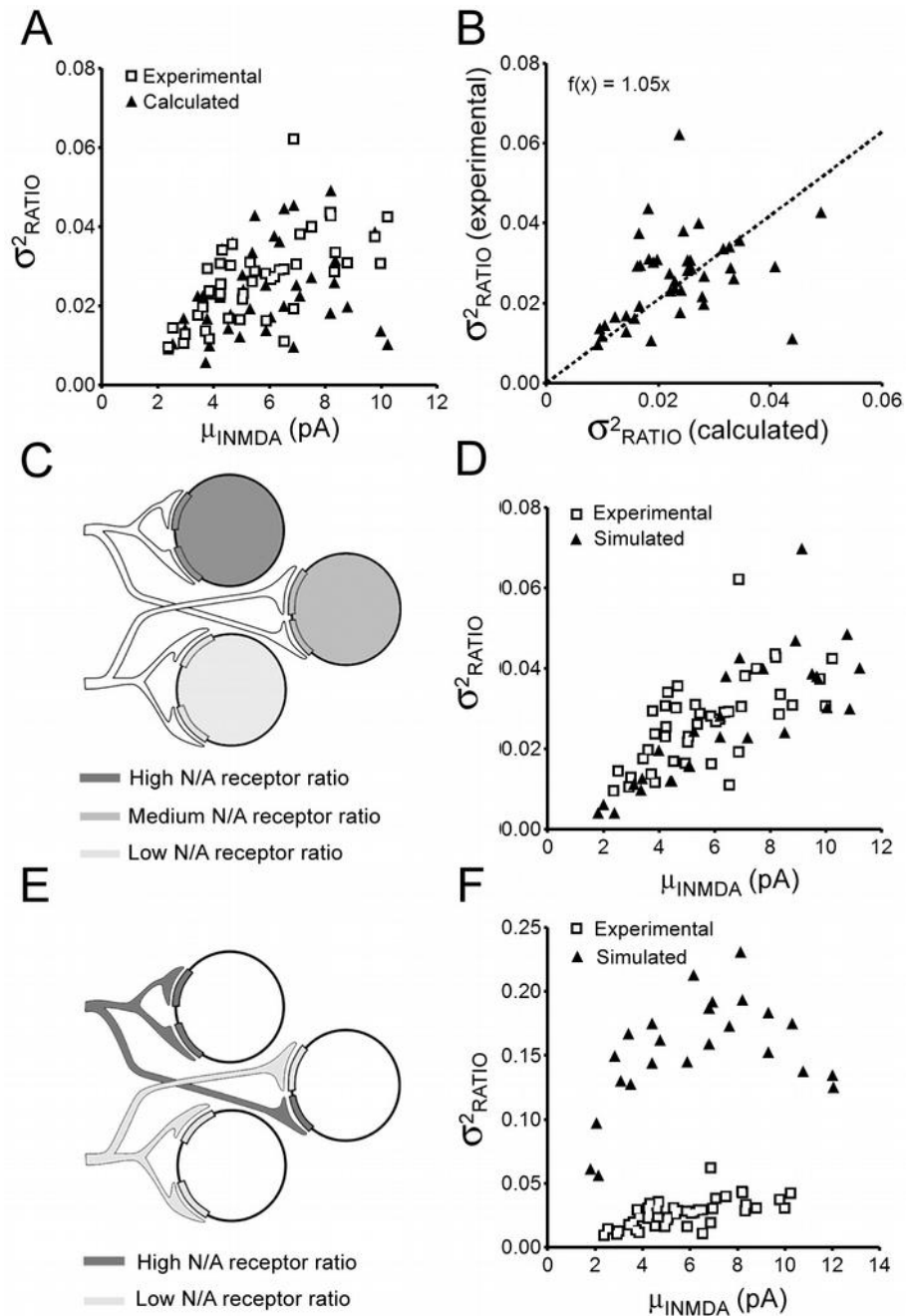


497 **Figure 2.A.** I_{NMDA} variance (σ^2_{INMDA}) across mEPSCs of recorded neurons as a function of mean I_{NMDA} .
 498 The solid line corresponds to NMDA receptor channel noise values predicted by equation 2 using a 50
 499 pS conductance and a 0.1 P_{op} value. **B.** I_{NMDA} variance in simulated mEPSCs series as a function of
 500 mean I_{NMDA} . Each data point represents a different mEPSCs series. Data were obtained using a constant
 501 amount of glutamate released (3000 molecules per quantal event). Note that the regression line of
 502 simulation values (dashed line) perfectly fits with NMDA receptor channel noise values predicted by
 503 equation 2 (solid line). **C and D.** As in B, except that the amount of glutamate released (3000
 504 molecules per quantal event on average for each series) was made variable from one quantal event to
 505 the other within each simulated mEPSCs series. The coefficient of variation of glutamate released was
 506 comprised between 0.26 and 0.31 in C and between 0.50 and 0.62 in D.



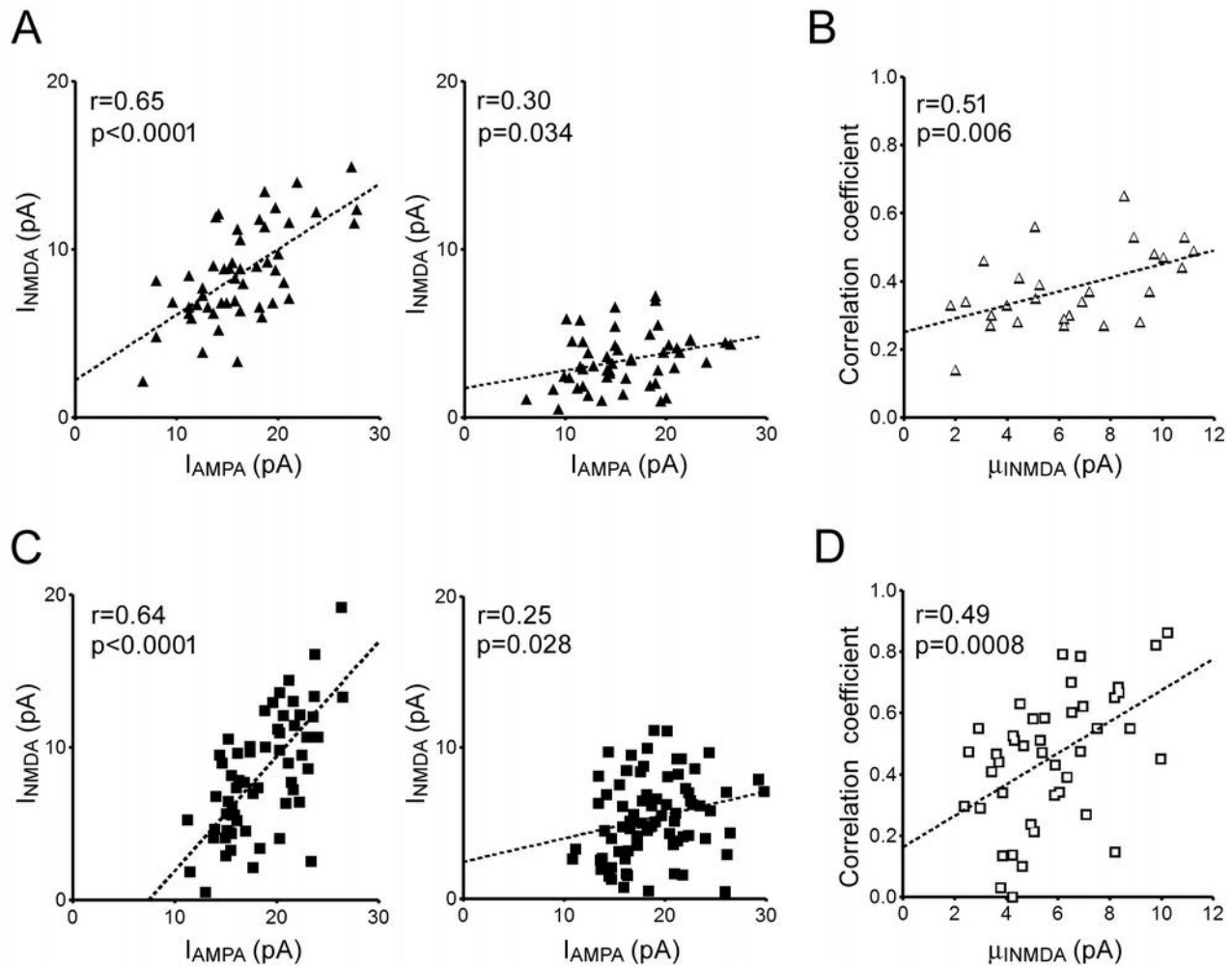
507 **Figure 3. A and B.** The influence of fluctuations in glutamate release on I_{AMPA} and I_{NMDA} variability.
508 Each data point represents the CV of I_{AMPA} (A) or I_{NMDA} (B) within a series of simulated mEPSCs
509 obtained with 100 AMPA receptors and 100 NMDA receptors and a fixed level of fluctuations in
510 glutamate release. Note the strong correlation between $CV_{I_{AMPA}}$ and CV_{Glu} and the lack of influence of
511 CV_{Glu} on $CV_{I_{NMDA}}$. **C and D.** I_{AMPA} (C) an I_{NMDA} (D) values in individual simulated mEPSCs plotted
512 against the amount of glutamate release. Note that the relationship with the number of glutamate
513 molecules released is strong for I_{AMPA} and considerably weaker for I_{NMDA} . **E.** I_{AMPA} variance in simulated

514 mEPSCs series obtained using a constant amount of glutamate released (3000 molecules per quantal
515 event). Each data point represents a different mEPSCs series obtained using either the kinetic scheme
516 from Robert et al. (2005) which includes a 20 pS conductance state and 7 and 14 pS subconductance
517 states (solid triangles) or a simplified kinetic scheme including a single 20 pS conductance state (empty
518 triangles). The solid line corresponds to AMPA receptor channel noise values predicted by equation 2
519 using a 20 pS conductance and a 0.23 P_{op} value. Note that subconductance states result in decreased
520 I_{AMPA} variance as compared to both expected channel noise and simulation values obtained using the
521 simplified kinetic scheme.



522 **Figure 4.A**. Variance of $I_{\text{NMDA}}/I_{\text{AMPA}}$ ratio across mEPSCs of recorded neurons as a function of mean
 523 I_{NMDA} . Note the overlap between experimental data (empty squares) and variances values recalculated
 524 for the same neurons using equation 4 (solid triangles). **B**. Regression of experimental ratio variance
 525 values on values recalculated using equation 4. The slope of the regression line (origin forced to 0,0) is

526 close to one indicating that I_{NMDA} contribution to ratio variability was mostly due to NMDA receptor
527 channel noise. **C.** Schematic representation of scenario 1 assuming identical NMDA to AMPA receptor
528 ratio across synapses onto the same target cell. Simulation was performed in 27 series (each
529 representing a different neuron) of 50 runs (each representing a different quantal event). The number of
530 AMPA receptor was set to 100 throughout runs and series. The number of NMDA receptors was
531 identical across runs within a series but increased from 10 to 100 across series. **D.** Comparison between
532 ratio variances obtained from recorded neurons (empty squares) and neurons simulated using scenario 1
533 (solid triangles). Note the strong overlap between the two sets of data. **E.** Schematic representation of
534 scenario 2 assuming different NMDA to AMPA receptor ratio across synapses onto the same target cell.
535 Simulation was performed in 27 series (each representing a different neuron) of 50 runs (each
536 representing a different quantal event). The number of AMPA receptor was set to 100 throughout runs
537 and series. The number of NMDA receptor was either 5 or 120 depending on the run. The proportion of
538 runs with 120 NMDA receptors increased (from 5:50 to 45:50) across series. **F.** Comparison between
539 ratio variances obtained from recorded neurons (empty squares) and neurons simulated using scenario 2
540 (solid triangles). Note that ratio variances obtained by simulation using different NMDA to AMPA
541 receptor ratio across synapses onto the same target cell were much higher than those obtained
542 experimentally.



543 **Fig. 5A.** Example of correlation between NMDA current amplitudes (I_{NMDA}) and AMPA current
544 amplitudes (I_{AMPA}) across quantal events from two neurons simulated using scenario1. Note the
545 difference in correlation strength between the two neurons. **B.** Relationship between μ_{INMDA} and I_{NMDA} -
546 I_{AMPA} correlation strength across neurons simulated using scenario 1. **C.** Correlation between NMDA
547 current amplitudes (I_{NMDA}) and AMPA current amplitudes (I_{AMPA}) across mEPSCs recorded from two
548 NTS projection neurons. **D.** Relationship between μ_{INMDA} and I_{NMDA} - I_{AMPA} correlation strength across
549 recorded neurons.